Fission barriers in the neutron-proton isospin plane for heavy neutron-rich nuclei

doi: 10.1103/PhysRevC.77.044308

Fission barriers in the neutron-proton isospin plane for heavy neutron-rich nuclei

F. Minato and K. Hagino
Department of Physics, Tohoku University, Sendai 980-8578, Japan
(Received 19 February 2008; published 14 April 2008)

We discuss the sensitivity of fission barrier for heavy neutron-rich nuclei to fission paths in the two-dimensional neutron-proton quadrupole plane. To this end, we use the constrained Skyrme-Hartree-Fock + BCS method, and examine the difference of fission barriers obtained with three constraining operators, that is, the neutron, proton, and mass quadrupole operators. We investigate ^{220}U, ^{236}U, and ^{266}U, that is relevant to r-process nucleosynthesis. We find that the fission barrier heights are almost the same among the three constraining operators even for neutron-rich nuclei, indicating that the usual way to calculate fission barriers with the mass quadrupole operator is well justified. We also discuss the difference between proton and neutron deformation parameters along the fission paths.

DOI: 10.1103/PhysRevC.77.044308 PACS number(s): 25.85.−w, 26.30.Hj, 27.90.+b, 21.60.Jz

I. INTRODUCTION

Fission plays a decisive role in determining the stability of heavy nuclei, where the Coulomb energy competes with the nuclear surface energy. Typical examples are superheavy elements (SHE). Although the fission barrier disappears in SHE in the liquid drop model, the nuclear shell effect leads to a relatively high fission barrier and eventually stabilizes SHE. The experimental efforts have been continued in many facilities to synthesize SHE using heavy-ion fusion reactions [1].

It has been well recognized that fission plays an important role also in the context of nuclear astrophysics [2,3], but systematic investigations on its role in r-process nucleosynthesis have started only in recent years [4–6]. The r-process is one of the most promising candidates for synthesizing the elements heavier than iron (Fe). In this model, nuclei capture a number of neutrons via successive (n, γ) reactions in a highly neutron-rich environment, e.g., neutron stars. As a consequence, the r-process path passes through the neutron-rich side in nuclear chart which cannot be reached experimentally at this moment. Heavy neutron-rich nuclei produced by the r-process may decay by spontaneous fission, neutron-induced fission, or beta-delayed fission [3–6]. The neutrino-induced fission might also play a role if the neutrino flux is significant [7]. In order to construct a reliable r-process model with fission, it is urged to calculate systematically fission barriers of many neutron-rich nuclei.

Theoretically, fission barriers can be calculated using either the macroscopic-microscopic model [8] or microscopic mean-field models [9–11]. In the latter approach, one selects a few important degrees of freedom for fission, such as quadrupole or higher multipole moments, and draws a fission energy surface using the constrained Hartree-Fock method with the corresponding constraining operators. The total energy is minimized with respect to all the other degrees of freedom than those considered explicitly in the calculation. In this sense, the mean-field approach provides an adiabatic potential energy surface for the case where the selected degrees of freedom are much slower than the other degrees of freedom so that they adiabatically follow the motion of the former at every instant.

Usually, one takes a mass (i.e., proton+neutron) quadrupole moment as one of the most important degrees of freedom. This implicitly assumes either that the isoscalar motion is much slower than the isovector motion or that the isoscalar and isovector motions are decoupled. For fission of neutron-rich nuclei, however, it is not obvious whether this assumption is justified, and it may be more natural that the shape degrees of freedom for neutron and proton are treated separately. In fact, a two dimensional energy surface spanned by proton and neutron deformations has been drawn recently for light neutron-rich nuclei, such as ^{16}C and ^{20}O [12–14]. The difference in neutron and proton deformation parameters along a fission path for actinide nuclei has also been investigated in Refs. [15,16].

In this paper, we examine the sensitivity of fission barriers for neutron-rich nuclei to a choice of constraining operator in the isospin plane. To this end, we use the constrained Skyrme-Hartree-Fock+BCS method, and consider the mass, proton, and neutron quadrupole moments as the constraining operators. The constrained Hartree-Fock method with the proton (neutron) constraint provides an adiabatic energy surface for the case where the proton (neutron) is much slower than neutron (proton).

The paper is organized as follows. In Sec. II, we use a schematic model and illustrate an example in which the constrained–Hartree-Fock method with the three different constraints give significantly different results from each other. In Sec. III, we briefly summarize the theoretical framework for constrained Skyrme-Hartree-Fock method. Section IV presents the results for the fission barrier, single particle levels, and the proton and neutron deformations along the fission paths for uranium isotopes. We then summarize the paper in Sec. V.

II. SCHEMATIC MODEL

In the constrained Hartree-Fock method with a constraining operator $\hat{O}$, one minimizes the expectation value of

$$\hat{H}' = \hat{H} - \lambda \hat{O}, \tag{1}$$

where $\hat{H}$ is the Hamiltonian of the system. The Lagrange multiplier λ is determined so that the expectation value of

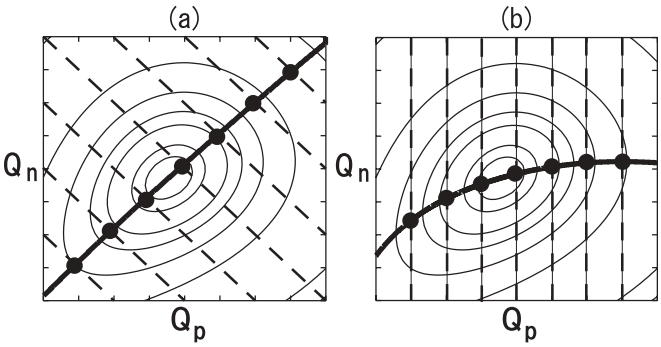

FIG. 1. Schematic pictures of the constrained Hartree-Fock method. Fig. 1(a) is for the total constraint, in which the energy is minimized along the lines of $Q_p + Q_n = const.$ shown by the dashed line. Fig. 1(b) is for the proton constraint, in which the energy is minimized along the lines of $Q_p = const.$ The corresponding paths are shown by the thick solid lines in both the figures.

$\hat{O}$ becomes a given value O_0. The $\hat{O}$ can be any one-body operator, but usually the mass quadrupole operator, $\hat{Q} = \hat{Q}_p + \hat{Q}_n$, where $\hat{Q}_p$ and $\hat{Q}_n$ are the quadrupole operators for proton and neutron, respectively, is considered as one of the constraining operators $\hat{O}$ when one studies fission barriers. The aim of this paper is to compare such fission barriers with those obtained by using $\hat{O} = \hat{Q}_p$ or $\hat{Q}_n$. We call the latter scheme "proton (or neutron) constraint" while the former "total constraint."

Before we perform self-consistent calculations, we would like to illustrate a possible difference among the three schemes for the constrained Hartree-Fock using a schematic model. Suppose that we have an energy surface shown in Fig. 1 in the two-dimensional plane of proton and neutron quadrupole moments, Q_p and Q_n. In the total constraint scheme, the energy minimum is searched along the line $\langle Q \rangle = \langle Q_p \rangle + \langle Q_n \rangle = \text{const.}$, which is shown by the dashed lines in the left panel. The resultant path is denoted by the thick solid line, and the energy variation along this path is shown in Fig. 2 by the solid line. In the case of the proton constraint, on the other hand, the energy minimum is searched along the dashed lines in the right panel of Fig. 1, which correspond to $\langle Q_p \rangle = \text{const.}$ The path and the energy are shown by the thick solid line in Fig. 1 and the dotted line in Fig. 2, respectively. The energy is plotted as a function of the total quadrupole moment along the path. Those of the neutron constraint are obtained in a similar way.

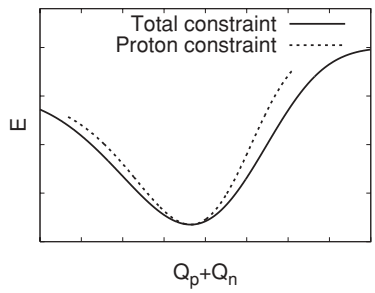

FIG. 2. The energy along the paths shown in Fig. 1. The solid and the dotted lines are for the total and the proton constraints, respectively.

We see clearly that the two paths obtained with the different constraining operators deviate significantly from each other. The energy is also different as a function of the total quadrupole moment, although the absolute minimum can be obtained irrespective to the choice of the schemes. The ambiguity arises when the number of the degree of freedom is reduced from two to one.

Notice that the differences among the schemes will be small if the energy surface is much steeper along the line of $\langle Q_p \rangle + \langle Q_n \rangle = \text{const.}$ In the next section, we will investigate how much the fission barriers are changed for realistic nuclei depending on which scheme one employs to minimize the energy.

III. NUMERICAL DETAILS

In order to calculate fission barriers for realistic nuclei, we use the Skyrme-Hartree-Fock+BCS method [17] (see Ref. [18] for a recent review). In this method, the expectation value of the Hamiltonian H is given in terms of an energy functional as

$$E = \int d\boldsymbol{r}\, \mathcal{H}(\boldsymbol{r}) \tag{2}$$

with

$$\begin{aligned}
&\mathcal{H}(\boldsymbol{r}) \\
&= \frac{\hbar^2}{2m}\tau(\boldsymbol{r}) + \frac{1}{2}t_0\left(\left(1+\frac{1}{2}x_0\right)\rho^2 - \left(x_0+\frac{1}{2}\right)\left(\rho_n^2+\rho_p^2\right)\right) \\
&\quad + \frac{1}{24}t_3\rho^\alpha\left((2+x_3)\rho^2 - (2x_3+1)\left(\rho_p^2+\rho_n^2\right)\right) \\
&\quad + \frac{1}{8}(t_1(2+x_1)+t_2(2+x_2))\tau\rho + \frac{1}{8}(t_2(2x_2+1) \\
&\quad - t_1(2x_1+1))(\tau_p\rho_p+\tau_n\rho_n) + \frac{1}{32}(3t_1(2+x_1) \\
&\quad - t_2(2+x_2))(\nabla\rho)^2 - \frac{1}{32}(3t_1(2x_1+1) \\
&\quad + t_2(2x_2+1))\left(\left(\nabla\rho_p\right)^2+\left(\nabla\rho_n\right)^2\right) - \frac{1}{16}(t_1x_1+t_2x_2)\boldsymbol{J}^2 \\
&\quad + \frac{1}{16}(t_1-t_2)\left(\boldsymbol{J}_n^2+\boldsymbol{J}_p^2\right) + \frac{1}{2}W_0(\boldsymbol{J}\cdot\nabla\rho + \boldsymbol{J}_p\cdot\nabla\rho_p \\
&\quad + \boldsymbol{J}_n\cdot\nabla\rho_n) + \mathcal{H}_C(\boldsymbol{r}).
\end{aligned} \tag{3}$$

Here, $\rho_q(\boldsymbol{r})$, $\tau_q(\boldsymbol{r})$, and $\boldsymbol{J}_q(\boldsymbol{r})$ are the nucleon density, the kinetic energy density, and the spin density, respectively, which are defined as

$$\begin{aligned}
\rho_q(\boldsymbol{r}) &= \sum_{i\in q,\sigma} v_i^2\,|\phi_i(\boldsymbol{r},\sigma,q)|^2, \\
\tau_q(\boldsymbol{r}) &= \sum_{i\in q,\sigma} v_i^2\,|\nabla\phi_i(\boldsymbol{r},\sigma,q)|^2, \\
\boldsymbol{J}_q(\boldsymbol{r}) &= (-i)\sum_{i\in q,\sigma,\sigma'} v_i^2\,\phi_i^*(\boldsymbol{r},\sigma,q)(\nabla\phi_i(\boldsymbol{r},\sigma',q)\times\langle\sigma|\boldsymbol{\sigma}|\sigma'\rangle).
\end{aligned} \tag{4}$$

In these equations, q denotes the isospin ($q = p$ or n), ϕ_i is the single-particle wave function, and v_i^2 is the occupation probability estimated in the BCS approximation. $\mathcal{H}_C(\boldsymbol{r})$ in Eq. (3) is the Coulomb energy term, while ρ, τ, and $\boldsymbol{J}$ are the total (proton+neutron) densities.

In this paper, we use the quadrupole operator

$$\hat{Q}_q = \sqrt{\frac{16\pi}{5}} \sum_{i \in q} r_i^2 Y_{20}(\theta_i), \tag{5}$$

as a constraining operator in Eq. (1). For simplicity, we assume the reflection and axially symmetric nuclear shapes, although the mass asymmetry sometimes plays an important role in describing nuclear fission. From the expectation value of the quadrupole operator, we calculate the total deformation parameter as [19]

$$\beta_t = \sqrt{\frac{5}{16\pi}} \frac{4\pi}{3AR_0^2} \langle Q_t \rangle, \tag{6}$$

where R_0 is the nuclear radius parameter given by $R_0 = 1.1A^{1/3}$ (fm). The proton and neutron deformation parameters are given by

$$\begin{aligned} \beta_p &= \sqrt{\frac{5}{16\pi}} \frac{4\pi}{3ZR_0^2} \langle Q_p \rangle, \\ \beta_n &= \sqrt{\frac{5}{16\pi}} \frac{4\pi}{3NR_0^2} \langle Q_n \rangle, \end{aligned} \tag{7}$$

respectively. The deformation parameters may be defined also in terms of the root-mean-square (rms) radius, instead of the constant R_0. We, however, prefer the present definition, Eqs. (6) and (7), since replacing R_0 with the rms radius does not necessarily improve an estimate of deformation parameter [19], on the contrary to what one would have expected.

In the actual numerical calculations shown in the next section, we use the computer code SKYAX [20,21]. This code solves the Skyrme-Hartree-Fock equations in the coordinate space with the reflection and axially symmetries. We use the mesh size of 0.6 fm. The pairing correlation is taken into account in the BCS approximation. In this paper, we use the delta force

$$v_{\text{pair}}(\boldsymbol{r}, \boldsymbol{r}') = -V_0\, \delta(\boldsymbol{r} - \boldsymbol{r}'), \tag{8}$$

for the pairing interaction. We expect that our conclusion is qualitatively the same even if we use a density-dependent delta interaction. In the code, the smooth cut-off function,

$$f_\alpha = \frac{1}{1 + \exp\left((\epsilon_\alpha - \lambda - \Delta E)/\mu\right)}, \tag{9}$$

is introduced for the pairing active space. Here, λ is the Fermi energy, and ΔE is determined so that

$$N_{\text{act}} = \sum_\alpha f_\alpha = N_q + 1.65 N_q^{2/3}, \tag{10}$$

with $\mu = \Delta E/10$, N_q being the number of particle for proton ($q = p$) or neutron ($q = n$). We use the strength parameter of $V_0 = 279.082$ MeV fm^3 for proton and 258.962 MeV fm^3 for neutron pairings [21].

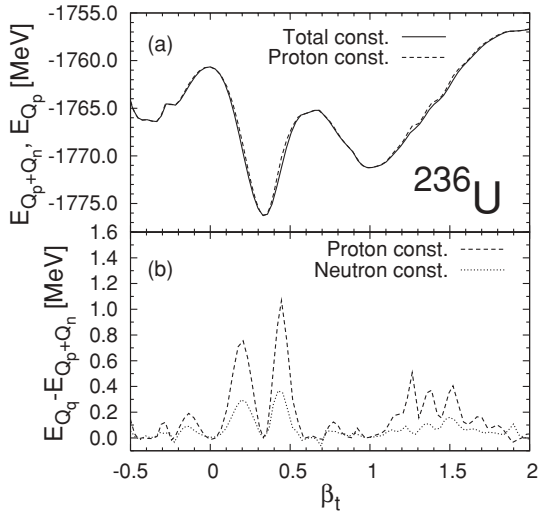

FIG. 3. The fission barrier for ^{236}U as a function of deformation parameter β_t obtained with the total constraint scheme (Fig. 3(a)). The dashed line in the Fig. 3(b) shows the difference of the fission barrier obtained with the proton constraint and that with the total constraint, while the dotted line denotes the difference obtained with the neutron constraint.

IV. RESULTS

We now present the results of constrained Hartree-Fock calculation for the fission barriers of ^{220,236,266}U nuclei. The ^{236}U is on the β-stability line, while ^{220}U and ^{266}U are proton-rich and neutron-rich nuclei, respectively. Notice that ^{266}U is relevant to r-process nucleosynthesis [22]. We adopt the parameter set SLy4 [23] for the Skyrme functional.

Figures 3 and 4 show the fission barriers for the ^{236}U and ^{266}U, respectively, as a function of the total deformation parameter β_t. The upper panels are obtained with the total constraint, while the lower panels show the difference of the fission barrier obtained with the proton constraint from that

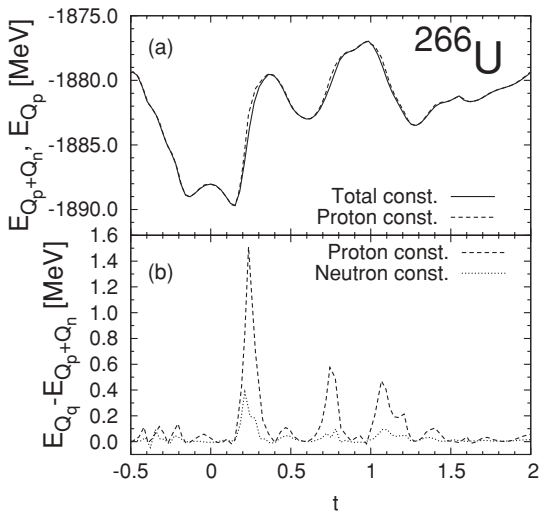

FIG. 4. Same as Fig. 3, but for ^{266}U.

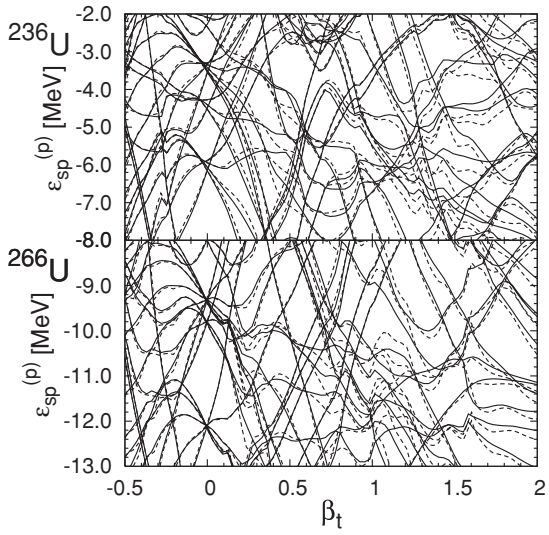

FIG. 5. Proton single particle levels near the Fermi energy for ^{236}U (the top panel) and ^{266}U (the bottom panel) as a function of the total deformation parameter. The solid and the dashed lines are the results for the total and the proton constraints, respectively.

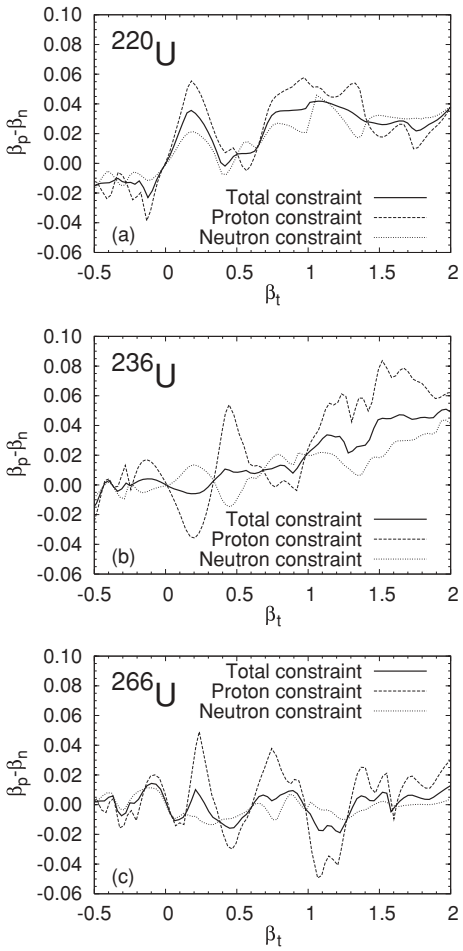

FIG. 6. Difference between the proton and the neutron deformation parameters, $\beta_p - \beta_n$, for ^{220,236,266}U nuclei as a function of the total deformation parameter. The solid, dashed, and dotted lines are the results for the total, proton, and neutron constraints, respectively.

with the total constraint (the dashed line). A similar quantity for the neutron constraint is also shown in the lower panels by the dotted line. The differences are much smaller than the fission barrier height, and the fission barriers obtained with the three schemes are almost indistinguishable in the scale shown in the figure. We have calculated for other even-even uranium isotopes from ^{220}U to ^{276}U, and confirmed that the three schemes lead to almost the same fission barriers for all of these nuclei.

Let us next discuss single-particle levels. Figure 5 shows the proton single-particle energies near the Fermi energy as a function of the total deformation parameter. The solid and the dashed lines show the results of the total and the proton constraints, respectively. We see that the single-particle energies are similar to each other between the total and proton constraints, although the difference is not negligible at large deformations. We have found that the tendency is similar also for the neutron constraints, although the deviation is smaller as compared to the proton constraint. We have also found that the conclusion remains the same also for the neutron single-particle energies.

The difference of deformation parameters for proton and neutron along the fission paths is shown in Fig. 6 for ^{220,236,266}U. Although the difference among the three curves is now more visible than in the fission barriers, the results with the three schemes are similar to each other, indicating that the fission path is not sensitive to the constraining operator in the isospin space. The $\beta_p - \beta_n$ is not a monotonic function of the total deformation parameter β_t, but on average it increases with β_t for ^{220}U and ^{236}U. Although the average value of $\beta_p - \beta_n$ appears to be zero even for large values of

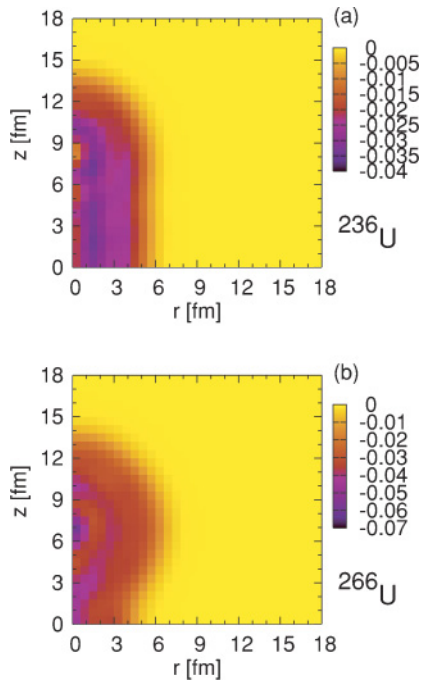

FIG. 7. (Color online) Difference of the proton and the neutron density distributions, $\rho_p - \rho_n$, for ^{236}U (Fig. 7(a)) and ^{266}U (Fig. 7(b)) at $\beta_t = 2.0$ obtained with the total constraint. The densities are axial symmetric around the z-axis.

β_t for the neutron-rich nucleus ^{266}U, this might be an artifact of using the same radius parameter R_0 between neutron and proton in Eq. (7) to calculate the deformation parameters (but see the discussion below).

Figure 7 shows the density difference of proton and neutron, $\rho_p - \rho_n$ for ^{236}U and ^{266}U obtained with the total constraint for $\beta_t = 2.0$. It is plotted in the two-dimensional plane of (r, z), where the density has the axial symmetric shape around the z axis. One can notice that the difference between the proton and the neutron densities is larger in ^{236}U than in the neutron-rich nucleus ^{266}U. This is consistent with the difference in the deformation parameter shown in Fig. 6.

V. CONCLUSION

We have used the constrained Skyrme-Hartree-Fock+BCS method with a quadrupole constraint in order to calculate the fission barriers of neutron-rich uranium nuclei with astrophysical interests. In particular, we carried out the calculations with the proton, neutron, and mass (total) quadrupole operators as the constraining operators. We have found that the fission barriers are almost independent of the constraining operators in the neutron-proton isospin space. We have discussed this behavior using a schematic model, and suggested that the potential energy surface is steep along the isovector degree of freedom. We have also found that the single-particle levels as well as the deformation parameters along the fission paths do not depend much on the constraining operators.

Our calculations indicate that the proton and the neutron deformations differ from each other even for the nucleus on the β-stability line, ^{236}U, and the difference increases as the total deformation parameter becomes large.

In the study of fission barriers based on the mean-field approaches, one usually uses mass multipole moments as constraining operators. Our results suggest that this approach is justified even for neutron-rich nuclei, where one might expect that the proton or neutron constraint is better. Of course, it is always desirable to treat proton and neutron separately for neutron-rich nuclei, and draw a two-dimensional fission energy surface. However, it is rather demanding to do so if one has to take into account explicitly many multipole moments, including simultaneously the quadrupole and octupole moments, or even higher multipole moments. Even in that case, our study clearly indicates that one can reduce the number of degree of freedom by introducing the mass multipole moments, rather than treating proton and neutron separately.

ACKNOWLEDGMENTS

We acknowledge the 21st Century for Center of Excellence (COE) Program "Exploring New Science by Bridging Particle-Matter Hierarchy" at Tohoku University for financial support. This work was partly supported by the Japanese Ministry of Education, Culture, Sports, Science and Technology by Grant-in-Aid for Scientific Research under program no. 19740115.

[1] *Proceedings of FUSION06: International Conference on Reaction Mechanisms and Nuclear Structure at the Coulomb Barrier*, edited by L. Corradi, E. Fioretto, A. Gadea, D. Ackermann, F. Haas, G. Pollarolo, F. Scarlassara, S. Szilner, and M. Trotta [AIP Conf. Proc. No. 853 (AIP, New York, 2006)].
[2] P. A. Seeger, W. A. Fowler, and D. D. Clayton, Astrophys. J. Suppl. **97**, 121 (1965).
[3] T. Kodama and K. Takahashi, Nucl. Phys. **A239**, 489 (1975).
[4] G. Martinez-Pinedo, D. Mocelj, N. T. Zinner, A. Kelić, K. Langanke, I. Panov, B. Pfeiffer, T. Rauscher, K.-H. Schmidt, and F.-K. Thielemann, Prog. Part. Nucl. Phys. **59**, 199 (2007).
[5] J. Beun, G. C. McLaughlin, R. Surman, and W. R. Hix, Phys. Rev. D **73**, 093007 (2006); arXiv:0707.4498 [astro-ph].
[6] I. V. Panov, E. Kolbe, B. Pfeiffer, T. Rauscher, K.-L. Kratz, and F.-K. Thielemann, Nucl. Phys. **A747**, 633 (2005).
[7] E. Kolbe, K. Langanke, and G. M. Fuller, Phys. Rev. Lett. **92**, 111101 (2004).
[8] P. Möller, D. G. Madland, A. J. Sierk, and A. Iwamoto, Nature (London) **409**, 785 (2001); P. Möller, A. J. Sierk, and A. Iwamoto, Phys. Rev. Lett. **92**, 072501 (2004).
[9] T. Bürvenich, M. Bender, J. A. Maruhn, and P.-G. Reinhard, Phys. Rev. C **69**, 014307 (2004).
[10] M. Warda, J. L. Egido, L. M. Robledo, and K. Pomorski, Phys. Rev. C **66**, 014310 (2002).
[11] M. Samyn, S. Goriely, and J. M. Pearson, Phys. Rev. C **72**, 044316 (2005).
[12] Nyein Wink Lwin, Ph. D. thesis, Tohoku University (2007).
[13] A. P. Severyukhin, M. Bender, H. Flocard, and P.-H. Heenen, Phys. Rev. C **75**, 064303 (2007).
[14] T. J. Bürvenich, Lu Guo, P. Klüpfel, P.-G. Reinhard, and W. Greiner, J. Phys. G: Nucl. Part. Phys. **35**, 025103 (2008).
[15] A. Dobrowolski, K. Pomorski, and J. Bartel, Phys. Rev. C **75**, 024613 (2007).
[16] J. F. Berger and K. Pomorski, Phys. Rev. Lett. **85**, 30 (2000).
[17] D. Vautherin and D. M. Brink, Phys. Rev. C **5**, 626 (1972).
[18] M. Bender, P.-H. Heenen, and P.-G. Reinhard, Rev. Mod. Phys. **75**, 121 (2003).
[19] K. Hagino, N. W. Lwin, and M. Yamagami, Phys. Rev. C **74**, 017310 (2006).
[20] P.-G. Reinhard, computer code SKYAX (unpublished).
[21] P.-G. Reinhard, D. J. Dean, W. Nazarewicz, J. Dobaczewski, J. A. Maruhn, and M. R. Strayer, Phys. Rev. C **60**, 014316 (1999).
[22] S. Goriely and B. Clerbaux, Astron. Astrophys. **346**, 798 (1999).
[23] E. Chabanat, P. Bonche, P. Haensel, J. Meyer, and R. Schaeffer, Nucl. Phys. **A635**, 231 (1998).